Journal of Non-Crystalline Solids 579 (2022) 121376

Contents lists available at ScienceDirect

Journal of Non-Crystalline Solids

journal homepage: www.elsevier.com/locate/jnoncrysol

Evaluation of the interaction of solar radiation with colored glasses and its thermal behavior

Teresa Palomar *, Esther Enríquez *

Instituto de Cerámica y Vidrio (ICV-CSIC), c/ Kelsen 5, Campus de Cantoblanco, Madrid 28049, Spain

ARTICLE INFO

Keywords:
Colored glass
Thermal impact
Thermography

ABSTRACT

Solar irradiation can induce different process on glasses. In this study, the thermal behavior of colored glasses (colorless, red, yellow, green, turquoise, blue, purple, and brown) were characterized by UV-vis-IR spectrophotometry, thermal conductivity-meter, infrared thermocamera and dilatometry. The calculation of the absorption coefficients and the thermal conductivity showed that the heating of each fragment depends predominantly on the chromophores. Blue, green and turquoise glasses present the highest NIR absorption, thermal conductivity, thermal expansion coefficient and the largest heating curve. In comparison with colorless glass, the expansion coefficient of bluish glasses is $> 5{\cdot}10^{-7}{}^{\circ}C^{-1}$ that can produce a thermal incompatibility with the formation of fissures and detachments.

1. Introduction

Colored glasses have been used in stained-glass windows since medieval age. Generally, they are formed by small colored pieces joined together by lead cames representing an iconography. These pieces can be painted with grisailles to create shadows or contours, or with enamels to introduce colors in the different glass fragments.

Stained-glass windows are generally exposed to environmental conditions (rain, wind, pollution…), which produce chemical alteration on the external side of the window [1–3]. Recently, thermographic studies have proved that the fragments can also experience a fast and intense change of temperature due to the impact of the sunlight [4]. During the monitoring, the temperature of the glass surface increased up to 10 °C in one hour, which can compromise the thermal stability of the window. Interestingly, the heating of stained-glass windows is not homogenous; it depends on the color, the thickness and the presence of paintings on each glass fragment [5–7]. Darker glasses show higher variations than lighter fragments. Grisailles and enamels can also interact with the sunlight producing punctual increases of temperature that are frequently related to surface detachments [6,8,9].

The color of each fragment depends directly on the chromophore. These elements can be ionic, molecular, colloidal or microcrystalline species. The most common chromophores are cations of the transition elements ($Mn^{2+/3+}$, Co^{2+}, $Fe^{2+/3+}$…). These ions interact with the light through the absorption of photons that permits to promote their valence electrons from the ground state into a higher energy orbital. The second group most common is formed by atoms or molecules in colloidal state that absorb and disperse the light, such as gold and copper ruby glasses. Finally, the less common group of chromophores is formed by large compounds such as particles of Cu_2O or Cr_2O_3 [10,11]. Each chromophore has a specific spectrum that depends on the electromagnetic configuration of the cations and the free energy levels in the uncompleted *d* orbitals of their electronic layer, or in the nature of the colloids/microcrystals and its concentration in the glass.

Additionally, colored enamels and grisailles can be used to decorate glass. These lead-glassy pigments are melted onto the glass during their manufacture. Grisailles are normally brownish or blackish pigments, instead of enamels which usually have a great palette of colors. These surface glassy pigments are particularly sensible to thermal variations [8,9]. As result, microfractures can be formed in the interchanged of both glasses that can induce their detachment. This phenomenon was particularly pronounced in the blue and green enamels.

Regarding the sunlight, it is formed by energy in the ultraviolet, visible and infrared region, but its electromagnetic spectrum is extremely variable because UV radiation can be filtered by cloud cover, pollution or air mass. Even, during the winter, the sun is lower in the sky and the radiation is filtered through a greater air mass than in summer [12]. Therefore, the interaction of sunlight with the glass chromophores can produce different phenomena. Chromophores interact with the visible light producing the glass color; but they can also interact with the

* Corresponding authors.
E-mail addresses: t.palomar@csic.es (T. Palomar), esther@icv.csic.es (E. Enríquez).

https://doi.org/10.1016/j.jnoncrysol.2021.121376
Received 21 September 2021; Received in revised form 19 November 2021; Accepted 22 December 2021
Available online 11 January 2022

ultraviolet (UV) and infrared (IR) radiation generating heating or light filtering. To study these interactions, and therefore, the thermal behavior of colored glasses, absorbance spectra measurement is an interesting tool since it allows to determine the amount of light absorbed in each region of the electromagnetic spectrum. However, it is important to note that to study the thermal heating of the glasses, it is necessary to take into account not only the light absorbed but also the capability to dissipate the heat produced by this absorption, which is mainly represented by the thermal conductivity. Thermal conductivity is hardly influenced by the phonon scattering, which are the responsible of the heat propagation. Therefore, a larger scattering of the phonons results in a worse heat propagation which reduces the thermal conductivity of the material. The phonon scattering may be produced by different effect, among them, a disordered structure, presence of different types of cations, defects, other phonons or a great number of grain boundaries [13]. However, it is important to note that the thermal conductivity mechanisms of glasses differ regarding a crystal material, due to its disordered lattice which produces anharmonic lattice interactions which are the responsible of the phonon propagation and strongly depends on the geometry of the structure. Therefore, the thermal mechanisms are more complex and difficult to understand, finding singular behaviors, such as a decrease in the thermal conductivity when the temperature decreases, and lower and spreader values of thermal conductivities [14–16].

Taking into account all these aspects, the aim of this work is to characterize the physical phenomena occurred when sunlight interacts with the colored glasses, depending on the chromophore ions, in order to understand the differential heating and degradation of the glasses. With this objective, an exhaustive study of light absorption and thermal conductivity in function of the glass chromophores has been carried out.

2. Methodology

2.1. Glass samples

The colored glasses were bought in LambertsGlas®. In order to identify the glass chromophores, the glasses were polished as slides with 1 mm of thickness. For the dilatometry, the samples were prepared in form of parallelepipeds of ~x223C1.3 cm length. Fig. 1 shows the picture of the thick glasses used.

2.2. Characterization techniques

The glasses were analyzed by X-ray fluorescence spectroscopy, dilatometry, UV-vis-IR spectrophotometry, thermal conductivity-meter, and infrared thermocamera.

Chemical analysis of the glasses was performed by X-ray fluorescence spectroscopy, using a Magic X 2400 spectrometer, PANalytical. The analyses were carried out using the semi-quantitative analysis curve of IQ+, analyzing the samples as a pearl (by melting 0.3000 g of sample and 5.5 g of $Li_2B_4O_7$).

UV-visible absorption spectra of original glasses and thin slides were recorded on a Perkin Elmer Lambda 950 UV/vis spectrophotometer. The illumination is a tungsten-halogen and deuterium light source in a double optical path covering the 200–2500 nm range with a resolution of 10 nm.

Bars were analyzed by dilatometry in a Netzsch DIL 402 PC/1 instrument at a heating rate of 5 °C/min. The coefficient of thermal expansion α (CTE) was obtained by a linear fit of the curve in the range 29–100 °C.

Thermal measurements were carried out by a DTC-25 conductivity-meter of TA Instruments using the guarded heat flow method at room temperature, and with electrodes temperatures of 40 °C and 10 °C. This method consists of placing the sample in contact with both electrodes and measuring how the temperature changes after a stabilization time, by means of 4 thermocouples. Glass samples have areas in the range of 3–9 cm^2 and thickness between 0.2 and 0.5 cm. The conductivity measurements were repeated 3 times, and the given values are the average of the three measurements.

Moreover, solar simulation experiments were performed by a LCS-100 solar simulator (Lasing S.A.) with a Xenon lamp of 100 W. The simulator possesses an AM1.5G filter (applied to the Standard G-173-03 with 1.5 air mass) that reproduces the solar spectrum with one sun equivalent power which allows measuring the reflective effect of the solar radiation on the samples. The solar filter is 81011-LCS with 2″ square AM0 filter mounted in frame. In addition, the solar simulation includes an AM1.5G spectral correction filter which shapes the light output to closely match the total (direct and diffuse) solar spectrum on the Earth's surface, at a zenith angle of 48.23 (ASTM E892). This provides a Class A irradiance spectrum suitable for photovoltaic testing. The surface heating was measured with a thermal infrared camera FLIR E30 which has an image resolution of 160 × 120 pixels and a temperature range of -20–350 °C with 0.1 °C of thermal resolution; and the rear heating was measured with a PT100 thermocouple connected to a multimeter Keithley 2410–1100 V, in voltage and current ranges of 0–100 V and 0–21 mA, respectively. The thermocouple system was calibrated using the cold focus method.

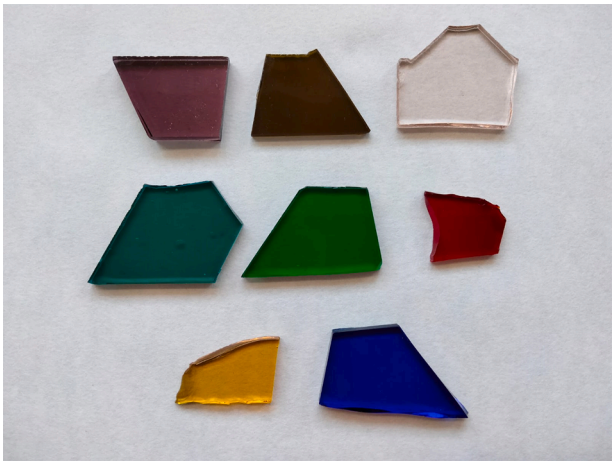

Fig. 1. Picture of the thick colored glasses bought in LambertsGlas®.

2.3. Solar simulation experiment

The heating experiment consists in irradiating the surface of the glasses with a solar simulator lamp in order to obtain their thermal behavior in the entire solar spectrum (280–2500 nm) with the corresponding contribution in each region (UV-Vis-NIR). Glass surfaces were irradiated during 10 min and then, the lamp was switched off (total 20 min). The achieved temperature on the surface during both the heating and cooling process was measured with an infrared thermocamera and, at the same time, temperature transmitted through the sample at the rear was measured by a thermocouple PT100 placed in the opposite size of the glass. The data obtained by the multimeter and the thermocamera was processed by a designed and a commercial software, respectively. Therefore, by this setup it was possible to obtain simultaneously heating curves in both sides of the sample with rather high resolution, which gives information about the absorption capacity and the in situ heat transfer through the sample, related with the thermal diffusivity. The experimental setup was previously reported [17] and was prepared as it is shown in Fig. 2 using the equipment described in the previous section.

3. Results and discussion

3.1. Glass characteristics

The glasses used in the present study are soda-lime silicate glasses

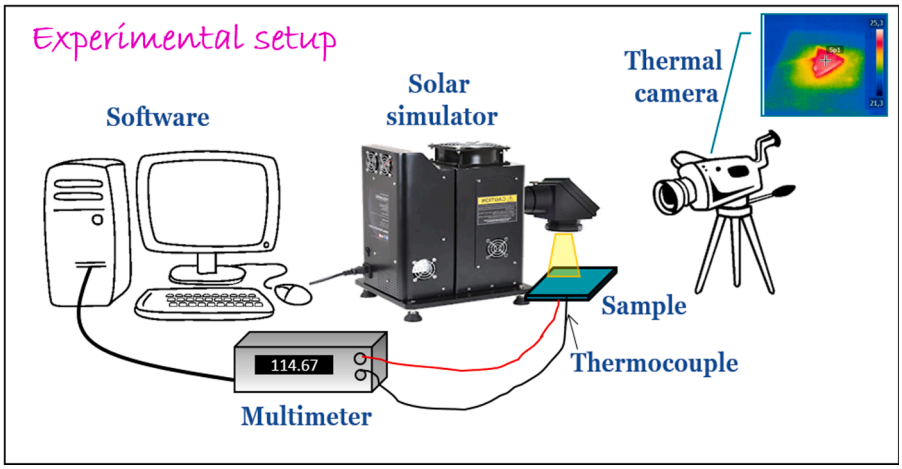

Fig. 2. Setup of the solar simulation experiment, where samples were irradiated during 10 min, and the heating at the surface and at the rear was measured by a thermal camera and a thermocouple, respectively.

Table 1
Chemical composition of the colored glasses.

	Chemical composition (wt%)							
	Colorless	Red	Yellow	Green	Turquoise	Blue	Purple	Brown
Na_2O	15.5	12.1	16.0	14.6	14.6	15.0	15.3	14.4
MgO	0.2		1.5	0.3	0.8	0.2	0.2	0.3
Al_2O_3	0.9	0.4	3.4	1.3	0.9	1.6	0.8	1.2
SiO_2	72.5	70.0	69.9	70.5	70.5	70.0	68.7	66.6
P_2O_5	0.1	0.1	0.1					
SO_3	0.1	0.1	0.1	0.2	0.2	0.2	0.2	0.1
K_2O	1.4	7.5	2.6	2.3	2.8	2.3	0.5	0.6
CaO	9.0	0.1	6.3	8.7	8.4	8.9	6.1	8.0
Cr_2O_3				0.3	0.1			
MnO							0.7	4.9
Fe_2O_3	0.2			0.1			0.1	3.7
CuO				0.4	1.1	1.8		0.2
ZnO		7.8						
As_2O_3	0.1			0.2				
CdO		0.3	0.2					
BaO		0.8		0.6	0.6			
PbO							7.4	

(Table 1). Nevertheless, they have different compositions in order to improve the characteristics of each coloration.

SiO_2 is the main former of these glasses together with Al_2O_3. P_2O_5, that appear in very low content, acts also as former, but commonly in glasses with optical characteristics due to its transparency in the UV and absorption in the IR region. P_2O_5 was detected in the red and yellow glasses (Table 1).

The alkaline oxides (Na_2O, K_2O) are fluxes that help to melt the glass at lower temperatures, and the alkaline-earth oxides (CaO, MgO, BaO) are stabilizers that avoid the glass degradation and the formation of crystallizations. Other oxides that act as stabilizers are PbO and ZnO, detected in those glasses with low content of alkaline-earth oxides.

Regarding the coloration, Cr_2O_3, MnO, Fe_2O_3 and CuO are species that give color to the glass through the absorption of frequencies in and near the visible region of the electromagnetic spectra (400–700 nm). The cations of the transition elements are the most common group of chromophores. The chromium ions give green color, manganese provide pink/violet color, iron contribute with a greenish hue and copper with a turquoise blue hue [4,10]. Concerning the cadmium, it can produce red/yellow coloration due to the synergic mechanism of absorption-dispersion of the light of colloidal or microcrystalline aggregations [10].

The arsenic oxide has been used along the history as decolorizing agent inducing the formation of Fe^{3+} with a pale yellowish hue; even it also favors the removal of glass bubbles during the glass melting.

The transmittance spectra represented in Fig. 3 show the bands of the chromophores in each glass. The colorless glass does not have bands in this range, probably because of the discoloration of the iron bands induced by the arsenic oxide.

The blue, turquoise and green glasses showed the wide single band of copper at ~x223C790 nm that enters in the IR region. The blue glass presented also the three bands characteristic from cobalt ion [4,18,19], which was under the detection limit of the XRF. Co^{2+}-ions have a high molar extinction coefficient, coloring the glass with a blue hue, even with low concentration.

The turquoise glass has the wide band of the copper together with a band at 450 nm, which could be related to the $^4A_2 \rightarrow {}^4T_1$ (F) transition of Cr^{3+}-ions in octahedral symmetry [4,20]. The other bands related to chromium could be overlapped with the wide band of the copper (Fig. 3).

The spectrum of the green glass showed the band of copper together with a very intense band at ~x223C370 nm and a shoulder at 420–440 nm that can be attributed to Fe^{3+}-ions in tetrahedral coordination. The XRF analysis detects Cr_2O_3, however, the bands of Cr^{3+}-ions could be overlapped with the iron and copper absorption bands (Fig. 3).

Regarding the purple glass, it is observed the broad band around 500 nm due to the Mn^{3+}-ions in octahedral coordination [21,22]. This band was also detected in the brown glass, together with bands of iron, cobalt and copper. The overlapping of all these bands produced a very complex spectrum (Fig. 3).

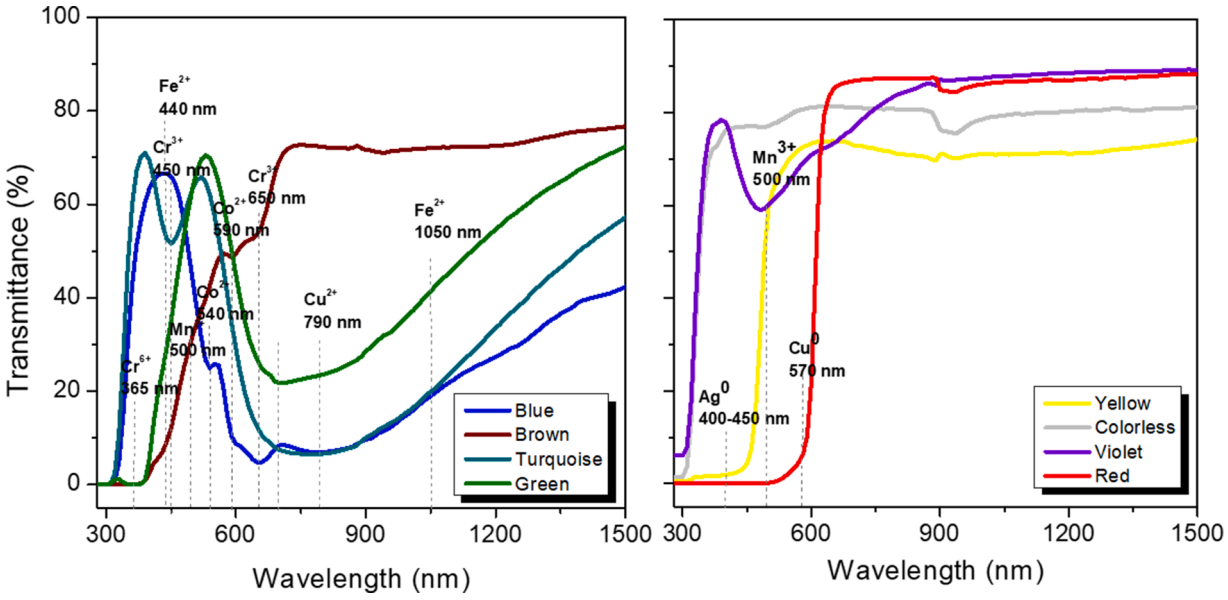

Fig. 3. Transmittance spectra of the (a) brown and bluish glasses and of (b) red, yellow, violet and colorless glasses (thin slides).

Finally, red and yellow glasses showed a slight red-shift (400–450 nm) (Fig. 3), which commonly depends on the Plasmon resonance of the colloids. The most common ruby glasses are those colored by gold, silver or copper; however, they were not detected by XRF (Table 1). This could be due because they were not used to color the glass or because their content was under the detection limit of the XRF. It was detected cadmium in both glasses (yellow and red), which suggests its use as chromophore. Colloids of cadmium selenide or sulfo-selenide can produce yellow and red glasses [10]. To obtain an intense ruby coloration, it is recommended to have > 18 wt.% of alkaline oxides and one third of them should be K_2O. Moreover, ZnO aids the stabilization of the ruby color [10]. The red glass composition satisfies these recommendations, proving that it was probably colored by cadmium. In case of yellow glass, only a small content of cadmium was detected and maybe could be colored by the same chromophore but with smaller colloids.

3.2. Thermal behavior of glasses

The solar spectrum is divided in three ranges with different contribution, 10% UV (200–400 nm) – 40% Visible (400–700 nm) – 50% Near Infrared (NIR) (700–2500 nm), where the UV is the most energetic range and NIR is the least one. Therefore, the light absorption in one or another region will produce different heating of the sample, that is, UV absorption would produce larger heating than NIR absorption; however, its contribution to the solar spectrum is much lower (only 10%). For this reason, it is important to study the absorption capability of the materials in each region, since it will influence in their heating. Moreover, absorption also depends on the sample thickness, since thicker samples will have higher absorption. Therefore, in order to normalize, the absorption coefficient is calculated following the Lambert-Beer law, $A = \alpha \cdot l$, where A is the absorbance, α is the absorption coefficient and l is the length of

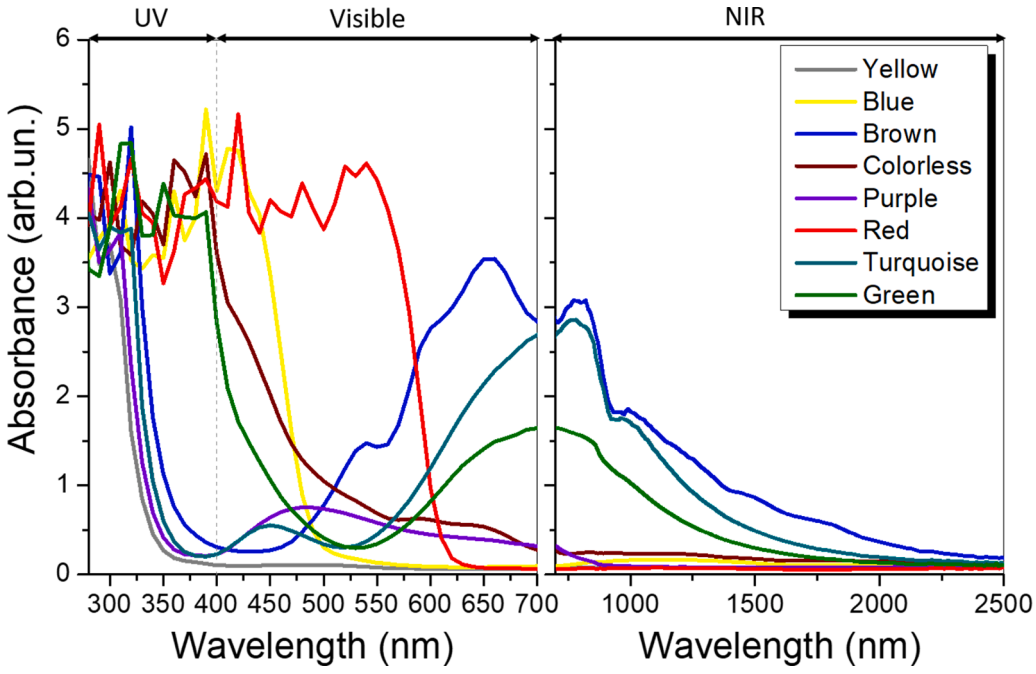

Fig. 4. Absorbance spectra of colored glasses in UV-Vis-NIR regions (thick samples).

light traveled [23]. Fig. 4 shows the absorbance spectra of all the glasses in the range 280–2500 nm. As seen, all samples have large absorption in the UV region, which is characteristic of glasses. In the visible range, the largest absorption corresponds to red, followed by blue and brown glasses. Finally, blue, turquoise and green glasses have the largest absorption values in the NIR region, being the rest practically transparent to infrared. Colorless and purple glasses have the lowest absorption values in all the spectrum. Table 2 shows the absorption coefficient values in each region and in the total spectrum for each glass, which correspond to the absorbance curves. As seen, blue glass possesses the largest total absorption coefficient, followed by turquoise, red and green glasses, and colorless and purple glasses have the lowest values. Therefore, according to these results, it is expected that the materials with highest absorption coefficient will be the most heated, that is, blue, turquoise, red and green glasses. However, the infrared is the heat-producing wavelength, so its absorption will strongly influence the material's heating. In agreement to this, red glass should be lower heated due to its low NIR absorption. To corroborate this presumption, thermographic studies have been carried out in order to determine the glasses heating when they are irradiated with a solar spectrum simulator.

Fig. 5 shows the thermal curves of the colored glasses registered with an infrared thermocamera when irradiated with the solar simulator during 10 min (continuous line), time at which the heating of the samples begins to stabilize. The thermal emission is registered in the infrared range, and therefore, a higher absorption of infrared light will produce a higher heating of the samples. At the same time, temperature of the rear part of the glasses is registered with a PT100 thermocouple (dotted lines) in order to determine the thermal propagation through the material. Both curves are normalized to the room temperature, showing the temperature gradient, that is the difference of temperature registered in each glass. Then the lamp was switched off and the cooling curves were also registered. As see, blue, green and turquoise glasses are the most heated under solar irradiation, with a gradient of almost 30 °C, which are the samples with the highest absorption in the NIR region (Table 2). Then, they are followed by brown (ΔT = 24 °C), red-yellow (ΔT = 16 °C), purple (ΔT = 14 °C) and colorless (ΔT = 10 °C) glasses, having the least NIR absorption in decreasing order (Tables 2, 3). Therefore, the heating of samples is highly influenced by the NIR absorption. This fact explains that although red glass has one of the highest values of total absorption coefficient (Table 2), it undergoes a lower heating, because its absorption in the NIR is very low. On the other hand, the thermal curves of the rear part (registered by the thermocouple) are very similar than in the front (registered by the thermocamera) for glasses with higher heating (blue, green and turquoise); however, in samples with lower heating, the rear part registers higher temperature than in the front. This difference of heating is due to the lower absorption by those glasses, according to the absorbance measures showed above, since the light passes through the sample in larger extent (larger transmittance), registering higher temperatures by the thermocouple at the rear. Therefore, the more the samples are heated (higher absorbance), the smaller the heating difference with the rear side. Fig. 5b shows the thermocamera images of the colored glasses taken after 10 min of irradiation. Images are placed in increasing order of heating, showing a difference of ~x223C 20 °C between the colorless and green-blue-turquoise glasses. The heating and cooling rates during the first 150 s were calculated in order to determine the heating and cooling tendency of each glass. This rate is correlated with the thermal conductivity and thermal diffusivity of the material, for this reason, thermal conductivity of samples was also measured (Table 3).

Table 2
Absorption coefficient values and thermal conductivity of colored glasses.

Color	Absorption coefficient (cm^{-1})			
	Total	UV	VIS	NIR
Colorless	0.05	0.46	0.03	0.02
Purple	0.05	0.36	0.12	0.02
Yellow	0.16	1.35	0.33	0.04
Brown	0.23	1.82	0.46	0.08
Green	0.25	1.35	0.33	0.16
Red	0.27	1.73	1.10	0.03
Turquoise	0.29	0.60	0.35	0.26
Blue	0.31	0.59	0.46	0.26

As seen, the heating and cooling rates of glasses coincide, which indicates that both phenomena are governed by the same thermal mechanisms. Samples with the highest heating rates are brown, green, blue and turquoise glasses, although the brown one stabilizes before, achieving lower temperature. On the one hand, the heating and cooling rates are influenced by the thermal conductivity, which is the capability of phonons (lattice vibrations) propagation through the material. Therefore, higher thermal conductivity, higher the heating rate. As is showed in Table 3, brown, green, blue and turquoise glasses possess the highest thermal conductivities, which correspond to the larger heating rates. The heating mechanisms that govern glasses are based on the interactions between the vibration modes. In a regular periodic lattice, the vibrations modes are as plane waves that can propagate indefinitely in an infinite medium. However, in a disordered lattice which produces anharmonic interactions, there are energy loss toward other vibration modes, and the normal modes are not as plane waves, but are the sum of several normal modes with different frequencies, which vary the free path way of the phonons. The introduction of some cations, such as $Fe^{2+,3+}$ or Cr^{3+} can modify these vibration mode, distorting the lattice, modifying the frequencies, and therefore the mean free path of the phonons, which will result in a variation of the thermal conductivity [14].

On the other hand, the thermal behavior is also influenced by the absorbance of the solar spectrum. Therefore, the differential behavior of the brown glass regarding the other three samples lies in that it possesses lower absorbance, especially in the NIR, achieving lower temperatures and stabilizing before. The heating mechanism are strongly influenced by the presence of multivalent chromophore ions. Particularly, iron and chromiun ions have strong absorption bands in the visible and near infrared ranges. Moreover, the oxidation states also influence the absorption of the glass, since for example, Fe^{3+} does not absorbs in the NIR but Fe^{2+} does [24]. Moreover, other authors explain how the increase of cobalt contained in the glass produces an increase in the thermal conductivity [25]. Therefore, glasses with these chromophores will have larger thermal conductivities. The other glasses have thermal conductivities up to two points lower and very similar each other, making them more thermally insulating, which is reflected in a lower heating rate (Table 3). This fact, joint to the lower absorption, especially in the NIR region, makes that these glasses achieve lower temperatures at lower heating rates, as well as a slowly cooling. These difference not only in the heating degree, but also in the heating and cooling rates, will strongly influence in the heat impact over the glass structure, as will see below.

3.3. Heat impact

The thermal expansion curves show that all the glasses have a similar behavior to thermal excitation (Fig. 6a). The red glass showed the lowest slope at high temperatures (200–500 °C) because its high content of ZnO (7.8 wt.%) decreases the coefficient of expansion of glasses. However, at low temperatures, the different colored glasses have similar coefficients of thermal expansion, having the colorless glass the lowest coefficient, followed by the reddish glasses (brown, purple, red, yellow), and finally the bluish ones (blue, green, turquoise) (Fig. 6b). This small difference in the coefficients can produce thermal incompatibilities if they are melted together, for example by fusing or by enameling. Two glasses are compatible when the difference of their expansion coefficients is lower than $5{\cdot}10^{-7}{}^{\circ}C^{-1}$ [10]. This difference can be reached with the colorless glass and the blue, green or turquoise glasses. This

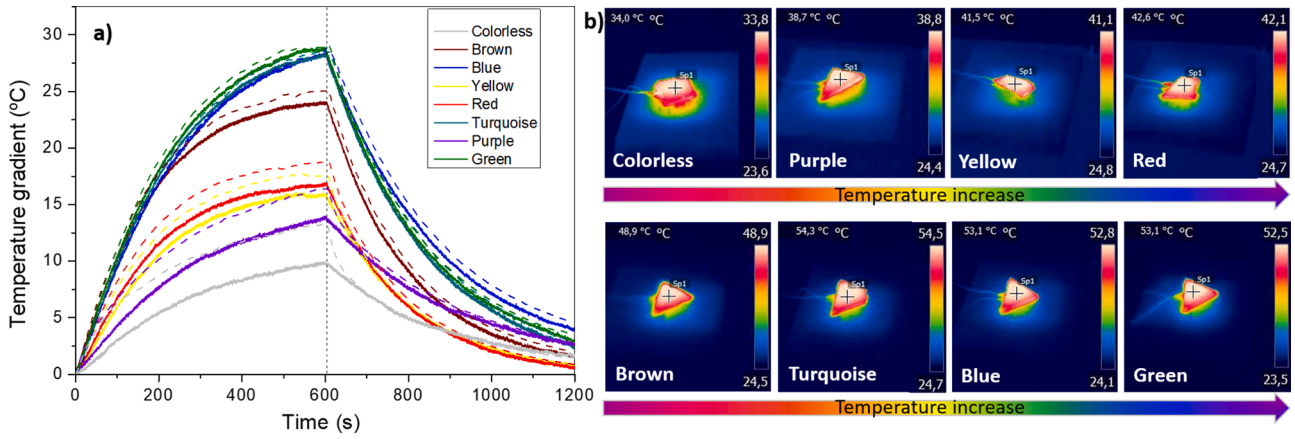

Fig. 5. (a) Heating and cooling curves of colored glasses when irradiating with a solar simulator during 10 min and then is switched off. (b) Thermocamera images of the colored glasses after 10 min of irradiation, placed in order of heating.

Table 3
Temperature gradients of heating curves, heating and cooling rates and thermal conductivity for colored glasses.

Color	Temperature gradient (°C)	Heating rate (°C/s)	Cooling rate (°C/s)	Thermal Conductivity (W/mK)
Colorless	9.9 ± 0.1	0.03 ± 0.01	-0.03 ± 0.01	0.65 ± 0.01
Purple	14.0 ± 0.1	0.04 ± 0.01	-0.04 ± 0.01	0.61 ± 0.01
Yellow	15.8 ± 0.1	0.06 ± 0.01	-0.06 ± 0.01	0.64 ± 0.01
Red	16.8 ± 0.1	0.07 ± 0.01	-0.07 ± 0.01	0.62 ± 0.01
Brown	24.0 ± 0.1	0.09 ± 0.01	-0.10 ± 0.01	0.74 ± 0.01
Green	28.7 ± 0.1	0.10 ± 0.01	-0.10 ± 0.01	0.81 ± 0.01
Turquoise	28.3 ± 0.1	0.10 ± 0.01	-0.09 ± 0.01	0.71 ± 0.01
Blue	28.4 ± 0.1	0.09 ± 0.01	-0.09 ± 0.01	0.88 ± 0.01

difference in the coefficient of linear thermal expansion together with the different heating/cooling curves (Fig. 5a) can compromise the stability of both glasses if they were melted together. During the solar irradiation, the bluish/greenish glass gets warmer, and, therefore, the expansion experienced by the colored glass could be higher than expected at the same temperature, forming stresses in the interface (Fig. 7). Repetitive cycles of heating/cooling can transform the stresses into fissures, and subsequently detachments on the colored glass. The most common detachments of historical windows are produced in blue and green enamels [8,26], which correspond to the glass with the largest NIR absorption, largest thermal conductivity, largest heating curve and highest thermal expansion coefficient, measured in this work. The presence of particles in the colored glass can accelerate this phenomenon [8].

4. Conclusions

The thermal behavior of different colored glasses has been analyzed. The glasses were soda-lime silicate glasses commonly used in restoration works. The chromophores of these glasses were cobalt, copper, chromium, iron, and, probably, colloids of cadmium selenide or sulfoselenide.

The absorption coefficients in the different regions (UV, VIS and NIR) were calculated from the absorbance spectra of colored glasses. Blue, turquoise, red and green glasses had the largest total absorption coefficients, and colorless and purple glasses the lowest values. However, only the bluish glasses had a high absorption in the NIR region, being the other glasses almost transparent to infrared.

The solar simulation experiment proved that blue, green and turquoise glasses are the most heated ones under solar irradiation, which are the glasses with highest NIR absorption. The red glass, with a high total absorption coefficient, was less heated due to its low NIR

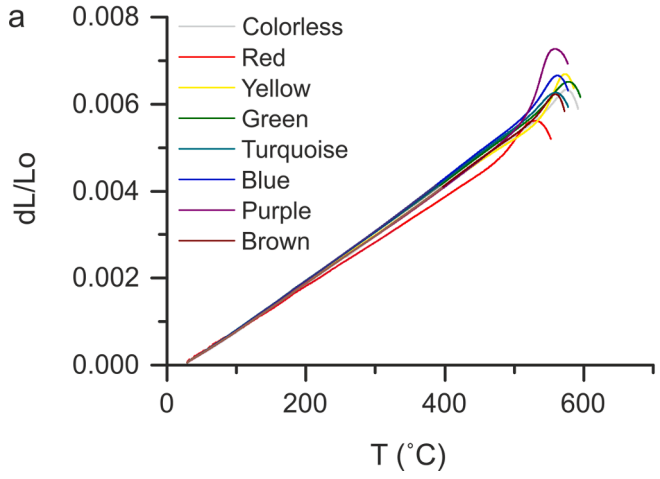

b

Color	$\alpha_{29\text{-}100\ °C} \cdot 10^7$ (°C^{-1})
Colorless	97.5
Red	101
Yellow	102
Green	104
Turquoise	105
Blue	103
Purple	100
Brown	100

Fig. 6. (a) Thermal expansion curves of the different glasses. (b) Values of the coefficient of linear thermal expansion (29–100 °C).

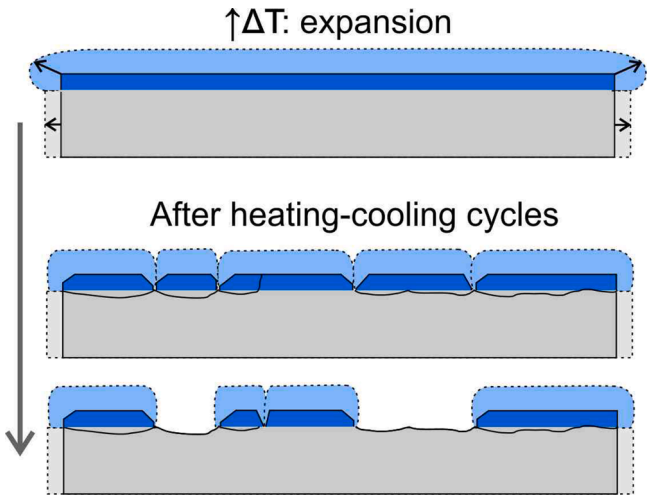

Fig. 7. Scheme of thermal incompatibility between two glasses melted together. Dot lines represent the glasses after expansion, and straight lines are fissures.

absorption. The bluish glasses also presented the highest values of thermal conductivity.

The coefficient of expansion of glasses are very similar between the different glasses; however, it is observed that in this case, blue, green and turquoise glasses have the highest values for the range 20–100 °C. These glasses have more than $5{\cdot}10^{-7}{}^{\circ}C^{-1}$ than the colorless glass, which could make them incompatible in case of being melted together, that can lead to detachment after several thermal cycles.

Credit author statement

TP designed the study; TP carried out the XRF, dilatometry and UV-vis-IR; EE made the thermal conductivity-meter study and the analysis with the infrared thermocamera; TP and EE prepared the original draft; all authors read and approved the final manuscript.

Availability of data and materials

All data generated or analyzed during this study are included in this published article. Raw data (including spectra) are available upon request from the authors.

Declaration of Competing Interest

The authors declare that they have no known competing financial interests or personal relationships that could have appeared to influence the work reported in this paper.

Acknowledgments

Authors acknowledge to Fernando Cortés (The Cathedral Studios, UK) for supplying the glass fragments. This work has been funded by the Fundación General CSIC (ComFuturo Programme) and the Spanish Research Agency (AEI, Ministry of Research and Innovation) (project MAT2017-86450-C4-1-R). We acknowledge support of the publication fee by the CSIC Open Access Publication Support Initiative through its Unit of Information Resources for Research (URICI). The authors also wish to acknowledge the professional support of the CSIC Interdisciplinary Thematic Platform Open Heritage: Research and Society (PTI-PAIS).

References

[1] T. Lombardo, C. Loisel, L. Gentaz, A. Chabas, M. Verita, I. Pallot-Frossard, Long term assessment of atmospheric decay of stained glass windows, Corros. Eng. Sci. Technol. 45 (2010) 420–424, https://doi.org/10.1179/147842210X12710800383800.
[2] T. Lombardo, L. Gentaz, A. Verney-Carron, A. Chabas, C. Loisel, D. Neff, E. Leroy, Characterisation of complex alteration layers in medieval glasses, Corros. Sci. 72 (2013) 10–19, https://doi.org/10.1016/j.corsci.2013.02.004.
[3] M. Melcher, R. Wiesinger, M. Schreiner, Degradation of glass artifacts: application of modern surface analytical techniques, Acc. Chem. Res. 43 (2010) 916–926, https://doi.org/10.1021/ar9002009.
[4] T. Palomar, C. Grazia, I. Pombo Cardoso, M. Vilarigues, C. Miliani, A. Romani, Analysis of chromophores in stained-glass windows using visible hyperspectral imaging *in-situ*, Spectrochim. Acta A 223 (2019), 117378, https://doi.org/10.1016/j.saa.2019.117378.
[5] T. Palomar, F. Agua, M. Gómez-Heras, Comparative assessment of stained-glass windows materials by infrared thermography, Int. J. Appl. Glass Sci. 9 (2018) 530–539, https://doi.org/10.1111/ijag.12352.
[6] C. Machado, A. Machado, T. Palomar, L.C. Alves, M. Vilarigues, Debitus grisailles for stained-glass conservation: an analytical study, Conserv. Patrim. 34 (2020) 65–72, https://doi.org/10.14568/cp2018067.
[7] T. Palomar, M. Silva, M. Vilarigues, I. Pombo Cardoso, D. Giovannacci, Impact of solar radiation and environmental temperature on Art Nouveau glass windows, Herit. Sci. 7 (2019) 82, https://doi.org/10.1186/s40494-019-0325-3.
[8] M. Beltran, N. Schibille, B. Gratuze, O. Vallcorba, J. Bonet, T. Pradell, Composition, microstructure and corrosion mechanisms of Catalan modernist enamelled glass, J. Eur. Ceram. Soc. 41 (2021) 1707–1719, https://doi.org/10.1016/j.jeurceramsoc.2020.10.041.
[9] F. Becherini, A. Bernardi, A. Daneo, F.G. Bianchini, C. Nicola, M. Verità, Thermal stress as a possible cause of paintwork loss in medieval stained glass windows, Stud. Conserv. 53 (2008) 238–251, https://doi.org/10.1179/sic.2008.53.4.238.
[10] J.M. Fernández Navarro. El vidrio, 3rd ed, Consejo Superior de Investigaciones Científicas. Sociedad Española de Cerámica y Vidrio, Madrid, 2003.
[11] W.A. Weyl, Coloured Glasses, Society of Glass Technology, Sheffield, UK, 1951. https://books.google.es/books?id=WBHwjwEACAAJ.
[12] P. Brennan, C. Fedor, Sunlight, UV, & accelerated weathering, Q-Lab Tech. Rep. LU-0822 (1994) 1–8.
[13] M. Zhao, W. Pan, C. Wan, Z. Qu, Z. Li, J. Yang, Defect engineering in development of low thermal conductivity materials: a review, J. Eur. Ceram. Soc. 37 (2017) 1–13, https://doi.org/10.1016/j.jeurceramsoc.2016.07.036.
[14] C. Kittel, Interpretation of the thermal conductivity of glasses, Phys. Rev. 75 (1949) 972–974, https://doi.org/10.1103/PhysRev.75.972.
[15] A.I. Krivchikov, A. Jezowski, Thermal conductivity of glasses and disordered crystals, ArXiv:2011.14728 [Cond-Mat.Dis-Nn]. (2020) 1–39.
[16] A.I. Krivchikov, O.A. Korolyuk, I.V. Sharapova, J.L. Tamarit, F.J. Bermejo, L. C. Pardo, M. Rovira-Esteva, M.D. Ruiz-Martin, A. Jezowski, J. Baran, N. A. Davydova, Effects of internal molecular degrees of freedom on the thermal conductivity of some glasses and disordered crystals, Phys. Rev. B Condens. Matter Mater. Phys. 85 (2012) 1–10, https://doi.org/10.1103/PhysRevB.85.014206.
[17] E. Enríquez, V. Fuertes, M.J. Cabrera, J. Seores, D. Muñoz, J.F. Fernández, New strategy to mitigate urban heat island effect: energy saving by combining high albedo and low thermal diffusivity in glass ceramic materials, Sol. Energy (2017) 149, https://doi.org/10.1016/j.solener.2017.04.011.
[18] C. Fornacelli, A. Ceglia, S. Bracci, M. Vilarigues, The role of different network modifying cations on the speciation of the Co^{2+} complex in silicates and implication in the investigation of historical glasses, Spectrochim. Acta Part A Mol. Biomol. Spectrosc. 188 (2018) 507–515, https://doi.org/10.1016/j.saa.2017.07.031.
[19] D. Möncke, M. Papageorgiou, A. Winterstein-Beckmann, N. Zacharias, Roman glasses coloured by dissolved transition metal ions: redox-reactions, optical spectroscopy and ligand field theory, J. Archaeol. Sci. 46 (2014) 23–36, https://doi.org/10.1016/j.jas.2014.03.007.
[20] A. Paul, Chemistry of Glasses, Springer Science & Business Media, London, 1989.
[21] N. Srisittipokakun, C. Kedkaew, J. Kaewkhao, P. Limsuwan, Coloration in soda-lime-silicate glass system containing manganese, Adv. Mat. Res. (2010) 206–209, https://doi.org/10.4028/www.scientific.net/AMR.93-94.206.
[22] C. Nelson, W.B. White, Transition metal ions in silicate melts-I. Manganese in sodium silicate melts, Geochim. Cosmochim. Acta 44 (1980) 887–893, https://doi.org/10.1016/0016-7037(80)90269-0.
[23] T.G. Mayerhöfer, S. Pahlow, J. Popp, The Bouguer-Beer-Lambert law: shining light on the obscure, ChemPhysChem (2020) 2029–2046, https://doi.org/10.1002/cphc.202000464.
[24] A.J. Faber, M. Rongen, A. Lankhorst, D.D.S. Meneses, Characterization of high temperature optical spectra of glass melts and modeling of thermal radiation conductivity, Int. J. Appl. Glass Sci. 11 (2020) 442–462, https://doi.org/10.1111/ijag.15111.
[25] S. Dalai, V. Savithri, P. Sharma, Investigating the effect of cobalt loading on thermal conductivity and hydrogen storage capacity of hollow glass microspheres (HGMs), Mater. Today Proc. 4 (2017) 11608–11616, https://doi.org/10.1016/j.matpr.2017.09.072.
[26] G. Van der Snickt, O. Schalm, J. Caen, K. Janssens, M. Schreiner, Blue enamel on sixteenth-and seventeenth-century window glass, Stud. Conserv. 51 (2006) 212–222.